PSEUDO-DUCTILITY BY FRAGMENTATION OF CENTRAL UNIDIRECTIONAL PLIES IN THIN CFRP ANGLE-PLY LAMINATES

J.D. Fuller*, M. Jalalvand, M.R. Wisnom

Advanced Composites Centre for Innovation and Science, University of Bristol, Queen's Building, Bristol, BS8 1TR

* *Corresponding Author: j.d.fuller@bristol.ac.uk*

Keywords: thin ply, delamination, pseudo-ductility, carbon fibre

Abstract

Pseudo-ductile metal-like tensile stress-strain responses with 700 MPa "yield stress" plateau and 4.0% failure strain have been achieved experimentally using thin-ply carbon epoxy prepreg and $[\pm 26_n/0]_S$ *(n = 8 and 10) layups. Analysis of tested specimens has been conducted using microscopy and ultrasonic C-scan. These show that periodic fibre breakages in the* $0°$ *plies lead to local delaminations that propagate along the* $0°/-26°$ *interfaces. This gradual failure process of fragmentation and dispersed local delamination allows the demonstrated pseudo-ductile strains.*

1. Introduction

The tensile responses of carbon/epoxy laminates have been usually reported to be linear elastic with a sudden final failure. But it has been shown in [1] that it is possible to produce non-linear stress-strain response with angle-ply laminates if the free edge delamination is suppressed using thin-ply technology. As part of the High Performance Ductile Composite Technologies (HiPerDuCT) programme, the current work aims to take advantage of the non-linear stress-strain response and damage suppression exhibited by thin ply angle-ply laminates [1] by combining these layups with unidirectional (UD) plies to improve the laminate modulus, yield stress and pseudo-ductile strain. 'Pseudo-ductility', in this case, refers to the geometric effect of fibre reorientation as well as yielding of the matrix. For clarity yield stress, σ_y, and pseudo-ductile strain, ϵ_d are shown graphically in Figure 1. The yield stress is defined as the point of intersection between the laminate stress-strain curve and a straight line of the initial modulus offset by 0.25 % strain. The pseudo-ductile strain is the failure strain minus the strain at the same stress level on a straight line of initial modulus.

Angle-ply laminate ply thickness has been studied in some detail [2, 3, 4, 5], showing that its reduction can increase the laminate strength [2], suppress damage in the form of matrix cracking and onset of free-edge delamination [3, 4, 6]. Reduction of the ply thickness below the industry standard of 0.125 mm was not viable at the time of the above research, due to the expense and difficulty of manufacture. The advent of novel tow-spreading processes e.g. [7] has allowed recent research [8, 9] to show that thin ply composites have the potential to possess higher strengths than standard ply thickness laminates and suppress damage to the point where delaminations due to open-hole tension and free-edge effects do not occur.

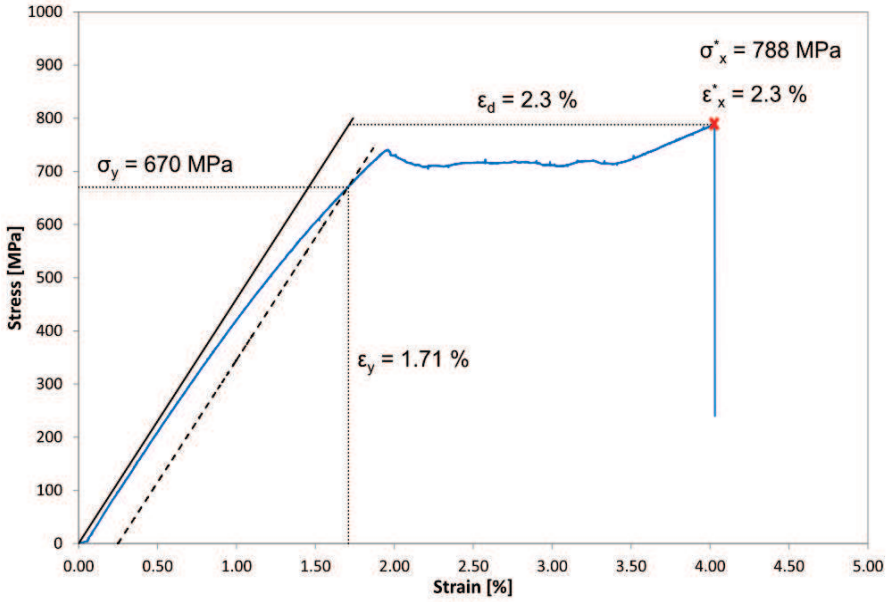

Figure 1. A graphical explanation of the method used to determine the yield stress and pseudo-ductile strain. The response shown is for a 1:8 laminate.

Other work within HiPerDuCT has demonstrated that pseudo-ductility can be achieved by hybridising UD thin plies of carbon fibre reinforced polymer (CFRP) with standard thickness glass fibre prepreg (GFRP) [10, 11]. Loaded in uniaxial tension, delamination is suppressed and fragmentation of the carbon ply occurs, leading to more gradual failure. It has been shown that the behaviour is very sensitive to the properties of each material and the thickness ratio between the low strain material (LSM), carbon, and high strain material (HSM), glass plies. The GFRP used to date, a standard 0.125 mm thickness material, has not permitted the desired fine adjustments of thickness ratio, thus limiting performance.

It is possible to remove this limit by using the thinnest available plies throughout the stacking sequence and combine the ply fragmentation and angle-ply rotation mechanisms for generating pseudo-ductile response. The material chosen is a Skyflex USN020A spread-tow CFRP, with a cured ply thickness of 0.03 mm, that has been used thus far in the angle-ply and hybrid laminates discussed. Use of the same material throughout, however, means that the laminate can not remain UD, as a difference between the strains to failure of the central and surrounding plies is required. To overcome this and to exploit their highly non-linear stress-strain behaviour, angle-ply layers are to replace the HSM GFRP plies. The high strains demonstrated by angle-ply laminates in previous work [1] make this configuration an excellent candidate for the high strain material required in these hybrid systems.

2. Test Methodology

2.1. Specimen Configuration

The test specimens were selected using the analytical method proposed in [12]. As previously mentioned, the behaviour of the laminate is dependent on the stiffness and thickness ratios between the LSM and HSM. These ratios can be readily assessed against each of the probable damage modes (shown in Figure 2) and a laminate configuration can be chosen. The graph of absolute LSM thickness versus relative LSM thickness produced for CFRP $[\pm\theta_n/0]_S$ laminates shows how the damage modes of overall delamination, sudden fibre failure and the desired frag-

No.	Order of required stress for damage modes	Expected damage process after the initial crack in the LSM		
1	$\sigma_{@LF} < \sigma_{del} < \sigma_{@HF}$	Fragmentation in LSM	Dispersed delamination	Failure of HSM
2	$\sigma_{@LF} < \sigma_{@HF} < \sigma_{del}$	Fragmentation of LSM	Failure in HSM	
3a	$\sigma_{del} < \sigma_{@LF} < \sigma_{@HF}$	Single delamination	Failure in HSM	
3b	$\sigma_{del} < \sigma_{@HF} < \sigma_{@LF}$	Single delamination	Failure in HSM	
4a	$\sigma_{@HF} < \sigma_{@LF} < \sigma_{del}$	Failure in HSM		
4b	$\sigma_{@HF} < \sigma_{del} < \sigma_{@LF}$	Failure in HSM		

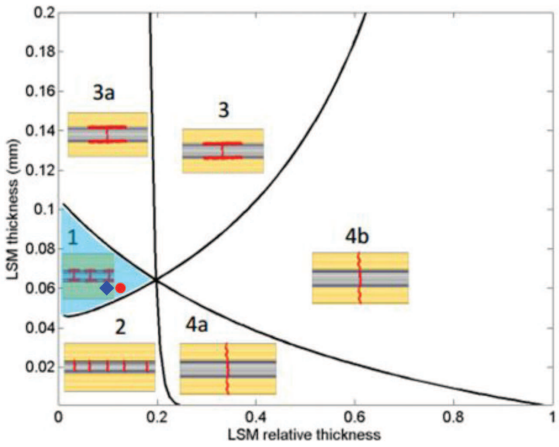

Figure 2. Table of expected damage modes (left) and map (right) showing how the absolute LSM thickness and thickness ratio between UD and ±26 plies influences these modes. The highlighted regions indicate the damage that is predicted for the current layups. Red circle and blue diamond show locations of 1:8 and 1:10 configurations respectively.

mentation with and without local delamination change with these laminate configurations. The highlighted regions (#1) show the damage process that is predicted by the analytical model. In this case, fragmentation of the UD plies should occur first, leading to dispersed, local delaminations of these central plies at the $0/-\theta$ interface, before final failure of the specimen.

E_{11}	101.7 GPa	E_{22}	6.0 GPa
G_{12}	2.4 GPa	ν_{12}	0.3

Table 1. Elastic properties of Skyflex USN020A.

Using the same Skyflex CFRP, previous work [1] has shown thin ply angle-ply laminates of $[\pm 26_5]_S$ exhibit relatively high strengths (> 900 MPa) and highly non-linear response with strains to failure > 4% in monotonic tensile loading, so this angle has been used in the present experiments. Skyflex material properties are shown in Table 1. The laminate configurations selected via the analytical method are: 1:8, that is one UD ply for every 4 pairs of ±26, and 1:10. Looking at the damage mode map in Figure 2, it can be seen that a minimum thickness of two UD plies (0.06 mm) is required to promote the desired behaviour. This leads to laminates of the following layups, with laminate thickness, t_p, shown in parentheses:

- $1:8 \Longrightarrow [\pm 26_4/0]_S \quad (t_p = 0.54mm)$
- $1:10 \Longrightarrow [\pm 26_5/0]_S \quad (t_p = 0.66mm)$

The specimen size chosen for the uniaxial tension tests performed had a gauge length of 150 mm and width of 15 mm, with glass-epoxy prepreg cross-ply end tabs of 40 mm. Five specimens of each layup were tested. The specimens were sufficiently long that ±26 fibres did not run from within one end tab to the other. Longitudinal and transverse strains were recorded using an Imetrum Video Extensometer and associated software, keeping target positioning consistent across all samples tested. All tests were performed using a Shimadzu 8800 mechanically-actuated machine, under displacement control at 2 mm/min.

3. Results

3.1. 1:8 Specimens

The stress - strain behaviour exhibited by the 1:8 specimens (Figure 3) was somewhat more unpredictable than anticipated. This may be explained by checking the position this configuration takes on the damage mode map (Figure 2). While the thickness of the central UD plies is constant for both 1:8 and 1:10, the thickness ratio is increased for 1:8 specimens. This moves the behaviour of the laminate towards the apex of the blue-shaded region - towards damage modes 4a and 4b. These modes predict a more sudden, catastrophic failure of the laminate, due to the lower thickness of $\pm\theta$ plies being transferred stress from the UD as it fragments. Any variation in the material, or specimen misalignment are likely to change the behaviour from one damage mode to another. These results, therefore, effectively expose a limit of exploitation for the current layup, since the laminate response can not be well predicted.

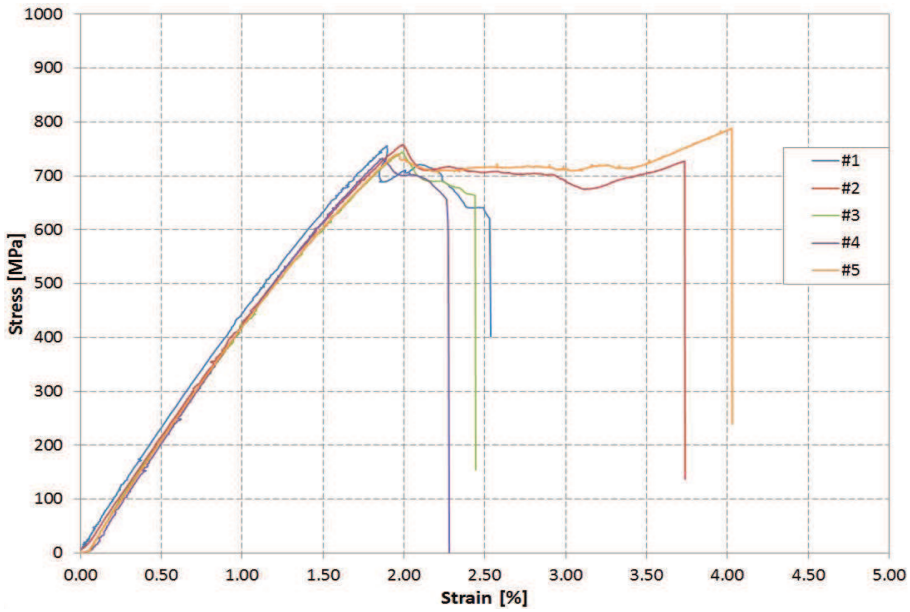

Figure 3. Stress - strain results for 1:8 specimens.

Parameter	1:8	1:10
Strength [MPa]	756.0 (3.2%)	801.2 (6.9%)
Yield Stress [MPa]	701.2 (5.2%)	691.7 (1.6%)
Failure Strain [%]	3.0 (27.2%)	4.2 (5.8%)
Pseudo-Ductile Strain [%]	1.3 (66.3%)	2.2 (7.4%)
Cured Ply Thickness [μm]	29.3 (0.4%)	

Table 2. Key results from 1:8 and 1:10 tensile tests. Values in brackets are coefficient of variation.

3.2. 1:10 Specimens

As Table 2 and Figure 4 both show, the stress-strain behaviour of the 1:10 specimens was much more consistent. All specimens show roughly linear initial loading, to the point at which the 0° layers begin to fragment. This occurs at the failure strain of these plies ($\sim$ 1.9%) and continues until the 0° plies are fragmented to the extent that they are unable to carry any increase in load. During this process, the stress is seen to be near constant, as the $\pm$26° plies are steadily

transferred stress from the UD layers. A section of reloading, at a lower modulus, is then seen. This portion of the stress - strain curve shows that the ±26° plies take up the further loading until complete failure of the specimen.

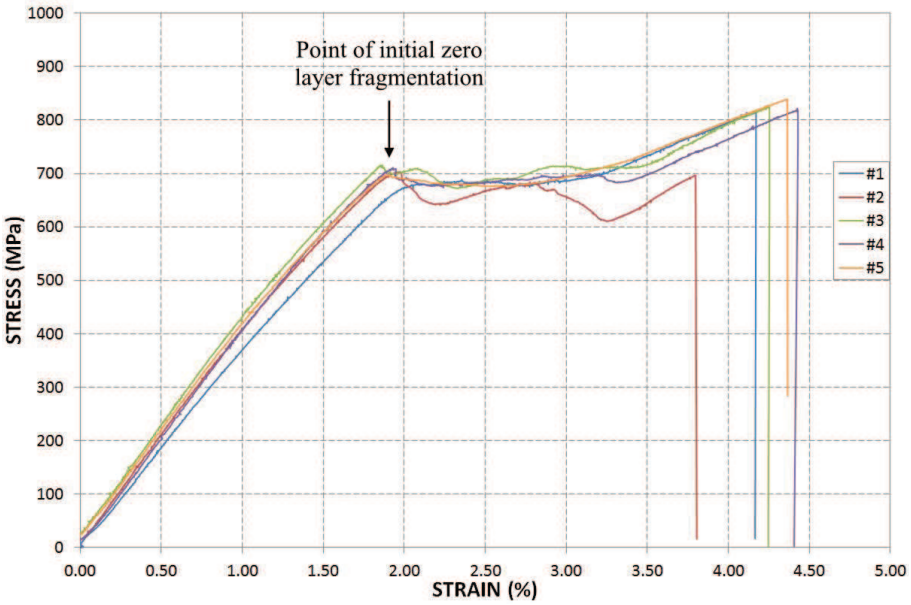

Figure 4. Stress - strain results for 1:10 specimens.

The stress plateau is shown by all but one of the specimens, (#2, red line), which exhibits an undulating path after the initial fragmentation of the 0° plies. The failure of the specimen also occurs much earlier, with the stress never exceeding the level of the first load drop. This behaviour could be down to poor set up in the test machine or a material defect. If treated as anomalous and removed from the sample, the mean strength and failure strain increase to 825.7 MPa (CV = 1.14%) and 4.31% (CV = 2.84%) respectively.

4. Analysis

4.1. Microscopy

Cross-sections of a $[\pm 26_5/0]_S$ sample have been made in order to help discern the damage process. Two micrographs of interest are presented here. This specimen has been loaded until near failure, so displays a high level of fragmentation in the 0° plies and some delaminations local to the fibre breaks at the 0/-26 interface. Figure 5 is a view of the free edge of the specimen, with enlargements showing the location and extent of fragmentations. Also highlighted by orange outlines, are the locations of delaminations that initiate from UD fibre breaks and then propagate along the 0/-26 interfaces, both above and below the 0° plies. It can be seen that these delaminations do not join up, indicating that some of the 0/-26 interface remains intact.

Whilst the periodicity of these fragmentations is not constant, there is some consistency in the spacing, which is typical of what is seen along the length of the laminate. The mean spacing over this section is 2.77 mm (min = 1.83 mm; max = 3.41 mm). This fragment spacing can be compared to the critical fragment length, l_c, using the equation below from [12], which relates the shear stress at the interface between the LSM and HSM to the strength of the LSM:

$$l_c = \frac{2\sigma_L t_L}{\tau_y} \tag{1}$$

Using values of fibre direction strength, σ_L = 1962 MPa, thickness of LSM, t_L = 0.03 mm and interfacial shear strength estimated from the in-plane value from $[\pm 45_5]_s$ tension tests, τ_y = 67 MPa, a critical length of 1.76 mm is found.

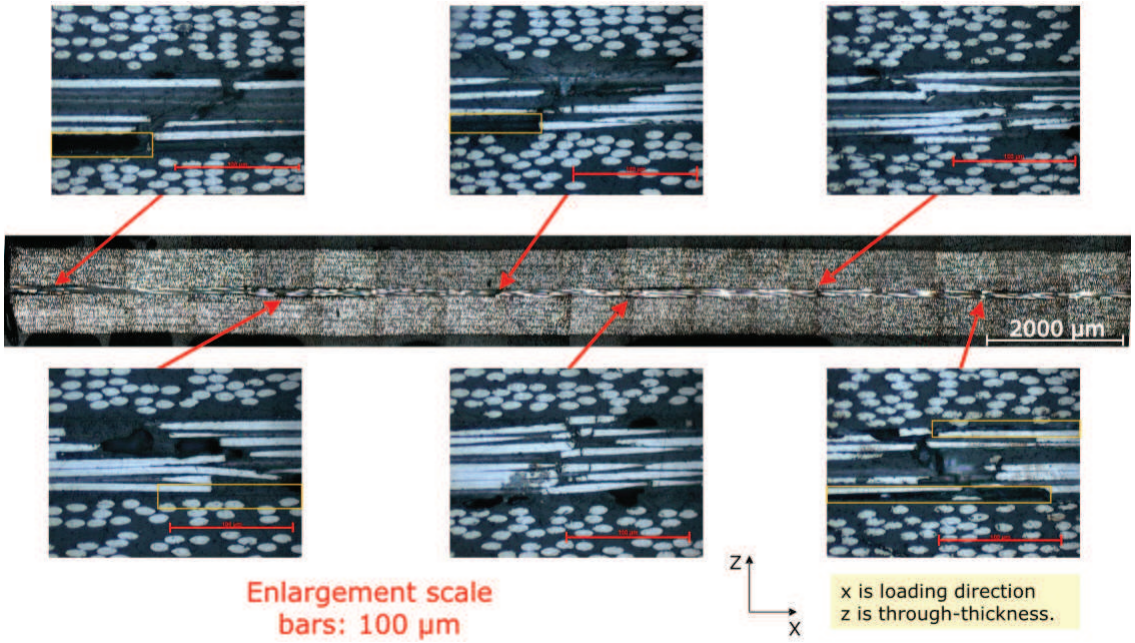

Figure 5. Micrograph shows free edge of specimen with enlargements indicating the positions of fragmentations in the 0° plies. Regions of delaminated 0/-26 interface are highlighted by orange boxes. Scale bar at bottom right corner of central image corresponds to 2 mm.

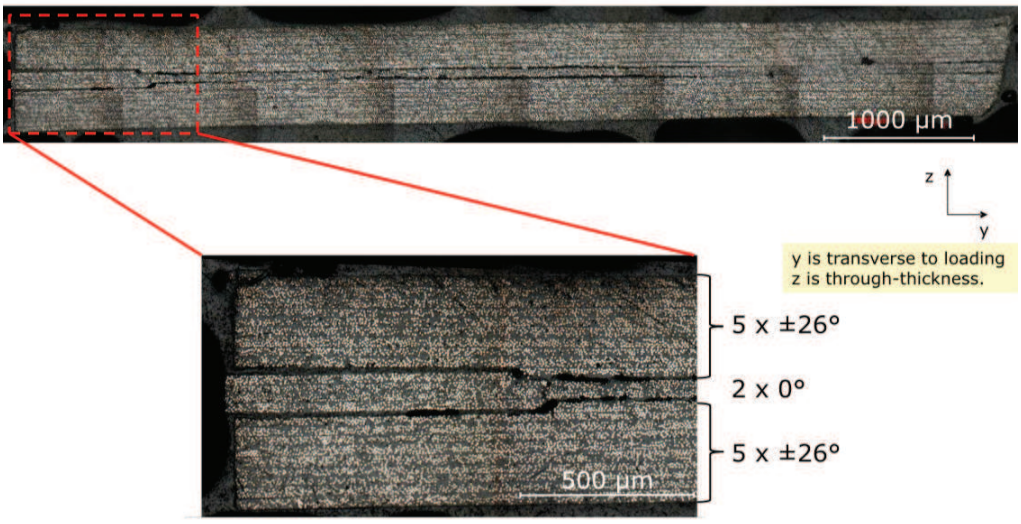

Figure 6. Micrograph shows extent of delamination across the width of the specimen. The symmetrical migration from the central 0° in to the adjacent −26° plies can clearly be seen.

Figure 6 shows a portion of the laminate cross-section, with the free edge on the left of both the main and enlarged images. This image shows that there is some delamination between the 0° and adjacent −26° plies, above and below, in the central region of the laminate (the right hand end of the image). These delaminations are seen to migrate through the −26° plies to the −26°/26° interface within 1 mm of the free edge of the specimen. In each micrograph taken of

different cross-sections of the laminate, a similar migratory behaviour is seen and in all cases this occurs in a symmetrical manner above and below the 0° plies.

Using the micrographs captured thus far, it is thought that the damage initiates from the fragmentation of the 0° plies. These cracks extend across the width of the specimen, with Mode II delaminations propagating either side of the fibre breaks. Free edge delaminations are also seen to occur at the $-26°/26°$ interface, seemingly independently of the fibre fragmentations. Visual inspection of tested specimens indicates that these delaminations are triangular in shape, similar to those commonly seen in angle-ply laminates. The migration of cracks seen in Figure 6 takes place when the local delaminations meet the ones propagating from the free-edge. This migration happens in the through thickness direction between the fibres. Propagation does not continue in to the next 26° ply, as fibres have to be broken for the crack to grow in this direction.

4.2. Ultrasound C-scan

One further $[\pm 26_5/0]_S$ specimen, also tested to near failure, has been analysed using a through-transmission scan with a 10 MHz ultrasonic probe. Microscopy has shown that delaminations originate from the fragmentation of 0° plies, so this method has been used to further aid the identification of damage in the laminate. The results, seen in Figure 7, show the strength of reflected wave in Volts. The darker areas indicate the weakest return, or heaviest attenuation, and the white a strong return. Delaminations represent an air gap in the composite and so heavily attenuate the ultrasound wave, thus identifying their position. These dark regions indicate that the damage in 0° plies extends across much of the sample, with only thin sections of the laminate remaining bonded.

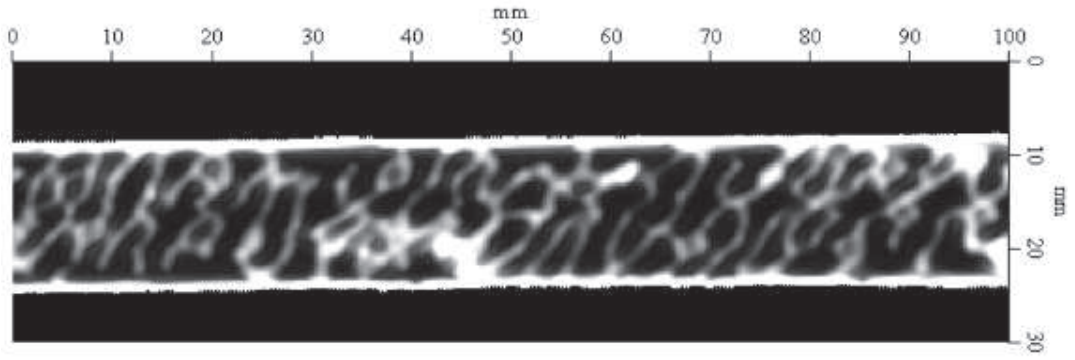

Figure 7. Image shows the amplitude level from a through-transmission ultrasound scan. The lighter areas indicate the regions of higher amplitude, pointing towards a lower level of attenuation. Possible delaminations are shown by the darker areas.

5. Conclusions

Laminates consisting of symmetric pairs of ±26° plies with 0° layers on the mid-plane have shown high performance pseudo-ductile results when quasi-statically loaded in tension. Two configurations have been tested, 1:8 ($[\pm 26_4/0]_S$) and 1:10 ($[\pm 26_5/0]_S$), following initial predictions indicating they may exhibit high pseudo-ductile strains after fragmentation and delamination of the 0° plies. The 1:8 specimens displayed unpredictable behaviour, three failing following the initial damage, but two showed higher strains to failure after a stress plateau and further loading of the undamaged ±26° plies. This behaviour, predicted to be proximal to the limit of the expected fragmentation and delamination, is thought to be a consequence of the variability in the material and non-linearity, which is not accounted for in the initial model. All 1:10 specimens showed impressive stress-strain behaviour, with a mean strain to failure of

4.21% and pseudo-ductile strain of 2.22%.

Damage was predicted to be fragmentation and then dispersed delamination of the central 0° plies, initiated at their strain to failure, 1.9%. These damage mechanisms have been shown, via microscopy and ultrasound scans, to be present. The order and rate of development of fragmentations, local and free-edge delaminations is subject to further work in order to better understand the damage process in these laminates.

Acknowledgement

This work is part of the EPSRC Programme Grant EP/I02946X/1 on High Performance Ductile Composite Technology in collaboration with Imperial College, London and is financially supported by grant number EP/G036772/1 (as part of the ACCIS Centre for Doctoral Training).

References

[1] J.D. Fuller and M.R. Wisnom. Damage Suppression in thin ply angle-ply carbon-epoxy laminates. In *The 19th International Conference on Composite Materials*, Montreal, 2013.

[2] C. T. Herakovich. Influence of Layer Thickness on the Strength of Angle-Ply Laminates. *Journal of Composite Materials*, 16(3):216–227, January 1982.

[3] A.S.D. Wang and F.W. Crossman. Initiation and Growth of Transverse Cracks and Edge Delamination in Composite Laminates Part 1. An Energy Method. *Journal of Composite Materials*, 14(1):71–87, January 1980.

[4] F.W. Crossman, W.J. Warren, A.S.D. Wang, and G.E. Law. Initiation and Growth of Transverse Cracks and Edge Delamination in Composite Laminates Part 2. Experimental Correlation. *Journal of Composite Materials*, 14(1):88–108, January 1980.

[5] T. Yokozeki, T. Aoki, T. Ogasawara, and T. Ishikawa. Effects of layup angle and ply thickness on matrix crack interaction in contiguous plies of composite laminates. *Composites Part A: Applied Science and Manufacturing*, 36(9):1229–1235, September 2005.

[6] R.Y. Kim and S.R. Soni. Experimental and Analytical Studies On the Onset of Delamination in Laminated Composites. *Journal of Composite Materials*, 18(1):70–80, January 1984.

[7] H. Sasayama, K. Kawabe, S. Tomoda, I. Ohsawa, K. Kageyama, and N. Ogata. Effect of lamina thickness on first ply failure in multidirectionally laminated composites. In *Proceedings of 8th Japan International SAMPE symposium and exhibition*, Tokyo, 2003.

[8] T. Yokozeki, Y. Aoki, and T. Ogasawara. Experimental characterization of strength and damage resistance properties of thin-ply carbon fiber/toughened epoxy laminates. *Composite Structures*, 82(3):382–389, February 2008.

[9] S. Sihn, R. Kim, K. Kawabe, and S. Tsai. Experimental studies of thin-ply laminated composites. *Composites Science and Technology*, 67(6):996–1008, May 2007.

[10] G. Czél and M.R. Wisnom. Demonstration of pseudo-ductility in high performance glass/epoxy composites by hybridisation with thin-ply carbon prepreg. *Composites Part A: Applied Science and Manufacturing*, 52:23–30, September 2013.

[11] G. Czél, M. Jalalvand, and M.R. Wisnom. Development of pseudo-ductile hybrid composites with discontinuous carbon- and continuous glass prepregs. In *16th European Conference on Composite Materials*, Seville, 2014.

[12] M. Jalalvand, G. Czél, and M.R. Wisnom. Damage mode maps and parametric study of thin UD hybrid composites. In *16th European Conference on Composite Materials*, Seville, 2014.